Partial discharge Source Calibration of Radiated Partial Discharge Signals

Adel Jaber
Azahra Higher Institute of Sciences and Technolog
Azahra- Libya
Jaber_ade@yahoo.com

Ehsan Altayef
Cardiff university
Cardiff School of Engineering
Cardiff,United Kingdom
altayefem@cardiff.ac.uk

Bdereddin Abdul Samad
Cardiff university
Cardiff School of Engineering
Cardiff,United Kingdom
AbdulSamadBF@cardiff.ac.uk

***Abstract*— Based on the IEC 60270 standard, a galvanic measurement and free-space radiometry (FSR) technique are used to measure partial discharge (PD) simultaneously. The PD source is a floating-electrode emulator type that was custom built. Sources are powered by AC or DC, power supplies. A biconical antenna captures the emitted a signal. The frequency band is derived from performing an Time-domain pulsing FFT analytics. The adjustment of a floating-electrode PD supply is focused for the advancement of a PD wireless sensor network (WSN).**

Keywords- Partial discharge; free space radiometric measurement; galvanic measurement; PD calibration.

I. INTRODUCTION

it is significant instrument the Measurement of PD in the checking and detecting in high voltage (HV) apparatus for insulation safety. by IEC 60270 standard then inductive/ bonding capacitively techniques the Partial discharge has usually been detected. The FSR exposure method of PD is a comparatively new way. The design that will be describe in this article to heading the standardization of a PD with floating electrodes origin wished for to expansion of a PD WSN.

II. APPARATUS

Figure 1 depicts the setup utilized to concurrently grasp FSR as well as galvanic detection methods.

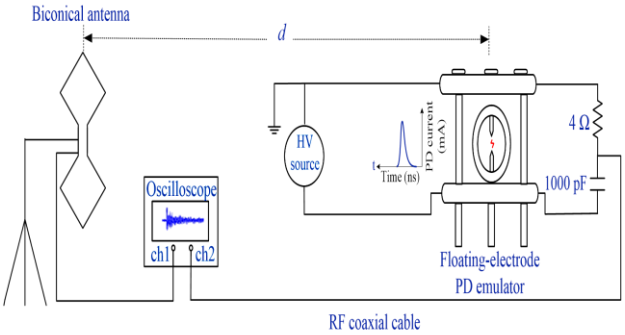

Fig. 1. PD gauge system.

The partial discharge is caused by stratifying an HV to a floating-electrode rival which is with 0.60 mm gap among floating electrodes and HV electrode. The FSR measurement was made by linking a 20 GSa/s, 4 GHz, Oscilloscope with digital sampling (DSO) to the biconical aerial. 2 m away from of the floating electrode emulator PD source the Antenna have being placed, and was perpendicularly polarized. Figure 2 demonstrations the biconical antenna schematic diagram [1]. The capacitor for conjugating voltage rating is 40 kV in galvanic size system. For PD a detecting, the floating-electrode emulator PD source with a parallel connection of coupling capacitors.

Frequency range: 20MHz to 1GHz
Max. input power: 5W AM (100MHz)
Nominal impedance: 50 Ohm
Gain : -9dBi at (100MHz)
RF connection: SMA socket (18GHz)
Calibration points : 196 (5MHz-steps)
Dimensions (L/W/D) : 540x225x225mm
Weight: 1150gr

Fig. 2. Biconical antenna.

Figure 3 is illustrated The floating-electrode PD emulator [2]. The HV output source of energy is linked to the bottom electrode while earth connected the higher floating electrode. Since there is an electrified area is appropriately charged a PD crown discharge is produced by the floating electrode. [3].

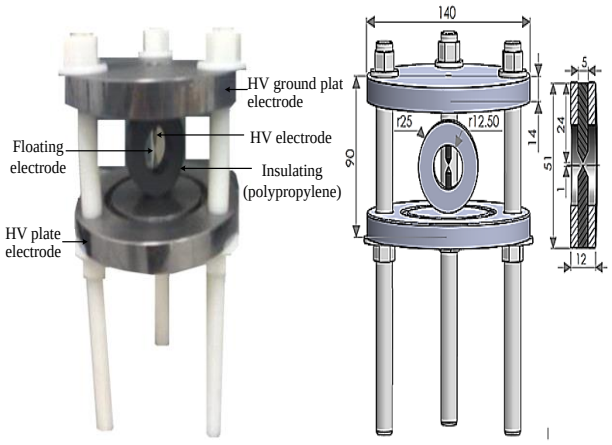

Fig. 3. Afloating electrode PD source (elements in mm).

A. *Example event*

The 2 dimensions techniques captured by the galvanic and FSR measurement, are presented in Figure 4. The HV that the PD event occurred was 6.2 kV. This occurrence exemplifies a number of comparable metrics. [4].

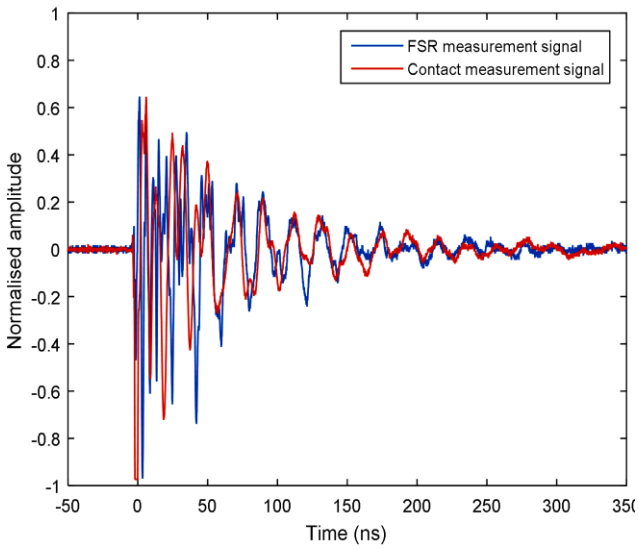

Fig. 4. galvanic and FSR Comparison of measures.

The decline of the two signals is comparable between the two observations. The degradation of the signals is close to what was expected. In the case of the photometric measurement system, severe band limitation of the test was predicted owing to electromagnetic waves and receiving mechanisms. In the case of the galvanic test, its less significant band limitation was expected. As a result, instead of the carrier frequency of the FSR reception antennas, band limitation is overcome by the inductance features of the PD source, capacitance, and linking wires. The frequencies bands demonstrate that the primary frequency of the PD discharge is between 50 and 290 MHz. However, the frequency spectra of galvanic and FSR measurements do not agree, with discrepancies in distribution systems as seen in Figure 5.

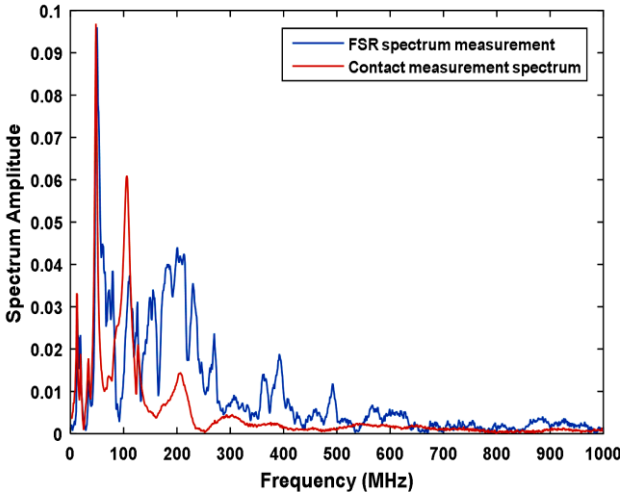

Fig. 5 The frequency spectra of galvanic and FSR data have been normalised.

III. PD CALIBRATION

The PD calibrator is an essential component of PD measuring equipment. It is necessary to go through a calibrating process. Measurement of a certain charge correctly The apparent charge can be set using the The calibrator induces a charge through into test circuit. The fee is specified using a formula. (1) and (2):

$$Q = \int_0^T i(t)dt \tag{1}$$

the Q is charge and i(t) is current.

The connection is formed when a current force is transferred to a voltage go down in a resistor.:

$$Q = \frac{1}{R}\int_0^T u(t)dt \tag{2}$$

where $u(t)$ is voltage and R is resistor.

The standard calibration procedure entails injecting a calibration pulse into the PD supply that is defined. Only off-line PD testing methodologies might well be calibrated as a result. The calibration technique is based on the assumption that the magnitude of the observed PD pulse is equal to the charge amount.

It is impossible to quantify partial discharge immediately. As condition, the charge amount is often taken from the outside circuit's measurable PD generated current pulse. This is known as the visible discharge, and it is normally obtained using one of two methods. A first method is to combine the time-domain PD pulse train. This is suitable for use in the labs, where the PD current pulse shape can be properly calculated, and interference is reduced to a negligible level. However, in the measurements made of the PD, the schemers are restricted because a lengthy synthesis time is required owing to resonance in the observed waveform PD current pulse and interference, which can make the integrating quality unintelligible. [5].

The second technique is through the calibration method recommended in the standard of the IEC60270. In this procedure, a calibration pulse with a known quantity of charge is inserted in to given test, and the proportion of the injected charge to the observed calibration pulse of the current or voltage magnitude is recorded. The PD calibration coefficient is the name given to this ratio. By multiplying the recorded PD pulse voltage or current magnitude by the PD calibration coefficient, the apparent discharge PD may be determined. This strategy might be used as long as the amplitude of the PD pulse is directly linked to the amount of charge.

A. HVPD pC Calibrator

An HVPD pC (picocoulomb) calibrator is an instrument that utilizes a PD generator to insert a predefined current pulse. The device is aimed to produce constant charge output at each setting has a temperature range of 1 pC to 100 nC and is suitable for PD experiments relating to the standard IEC 60270. The HVPD pC may be utilised in on-site testing and laboratory environments. The device calibrator may be accustomed to evaluating each kinds of high voltage apparatus of power distribution systems and

compute the visible charge's PD magnitude that used a diverse selection of calibration pulses. Figure 6 demonstrations off-line high voltage pC calibrator [12].

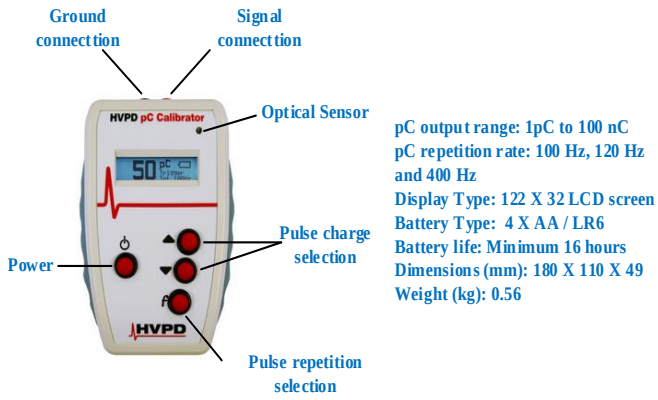

Fig. 6. HVPD pC calibrator with specification.

B. Partial Discharge Source Calibration

To determine the severity of a partial discharge, the actual charge conveyed during the discharge occurrence is relied to. It is generally measured in pico-coulombs (pC) or nano-coulombs (nC) and is proportional to the current's time total pulse. The seeming charge is the energy that, when administered into the communication resources under examination, gives the same measurement device response as the PD event [13].

As mentioned in [14], most PD tests use a galvanic link to send the PD current pulse (or a current pulse proportional to a voltage pulse) across a line to the measurement instrument.

The visible charge in this example was discovered using an integrated pulse. However, it is hard to assess radiated PD intensity in this manner because the RF signal at the endpoints of a receiving antenna is often connected to the PD current pulse time derivative rather than a time integral. Furthermore, inside the situation of multispectral detected PD, there are different transmission losses that are generally unexplained, such as the reflection coefficient of the propagation losses and the transmitting structure.

Figure 7 shows the effects of injecting a known charge amount into a DSO. The analyzer has a one-million-ohm input impedance. By incorporating the first half of the cycle of the PD supply series data current, the charge is computed (observed charge) and/or the top voltage of the FSR reading in comparison to the calibrator's stated charge (insert charge). the charge injection device, as well as the charge estimated from the galvanic magnitude, appear selected a valid method of calibrating PD suppliers.

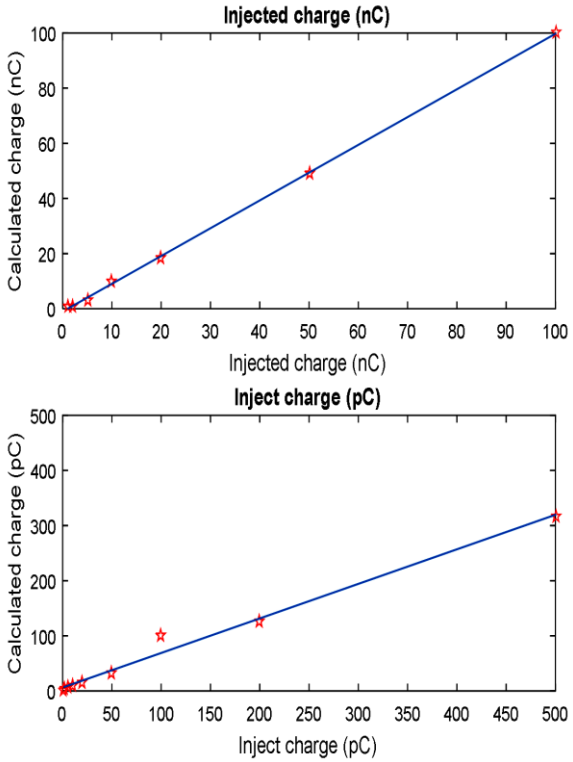

Fig. 7. Charge was calculated by integrating the initial fifty magnitudes of pulses against input charge..

Table 1 the connection between both the inserted charge and the computed charge

Pulse charge injection	Integration time of initial half-cycle of the PD source (ns)	charged determined	Top voltage of calculated charge (V)
50 pC	48.0	50.8 pC	0.013
100 pC	47.4	119 pC	0.04
200 pC	48.4	206 pC	0.03
500 pC	45.2	544pC	0.10
1 nC	47.6	1.5 nC	0.34
2 nC	46.4	1.6 nC	0.21
5 nC	44.3	5 nC	0.88
10 nC	46.5	16 nC	3.32
20 nC	85.5	14 nC	0.96
50 nC	84.6	35 nC	2.77
100 nC	83.1	72 nC	5.77

See figure 8 a known charge amount of calibrator is inserted into terminals of PD simulator with floating electrodes. The waveform as seen in figure 9 by injected charge of galvanic measurement pulse is observed.

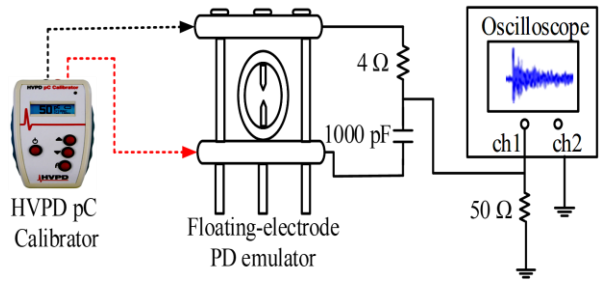

Fig. 8. Experimental measuring circuit measurement.

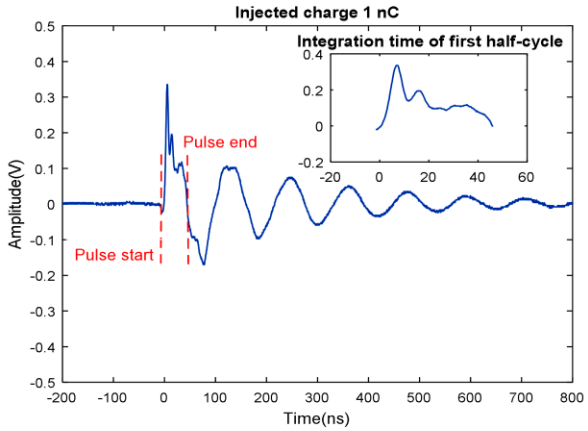

Fig. 9. A current curve with an inserted charge of 1 nC is shown as an example.

The results in Table 1 demonstration the quantity among input charges that is injecting current pulse by HVPD calibrator and the output is the calculated charge pulse of the PD emulator. In addition, it shows the peak voltage of charge calculated (measured charge). Nevertheless, This became impossible to tell the difference between the signals obtained from the 1 pC to 20 pC discharges or from the ambient noise. the charge calculated as illustrated in Figure 10, by combining its first side of the cycle of the PD simulator data series applied current energy to against calibrator's determined charge (inserts charge).

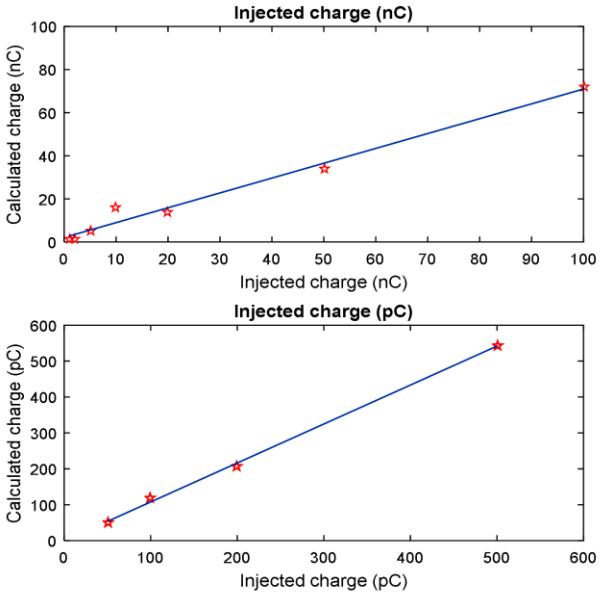

Fig. 10. Compute the load vs the stated charge of the electrode potential unit.

Testing AC HV power source across the floating electrode PD emulator at varying distances among the PD emulator along with the antenna utilized the size method see Figure 1. One waveforms of galvanic measurement signals and four waveforms of FSR signals were verified at 15 kV HV of power source. Table 2 shows the AC HV, versus the received mean range of the maximum voltage, calculated charge and FSR measurement's generated output energy. distance among the source code for the PD driver and the antenna was 1m, 2m, 3m and 4m. Lowering the amplitude of the signals by increasing distances in the middle of the PD emulator supply location and antenna, owing to the emission. Two techniques are provided to calibrate FSR measurement signal. The effective radiated power (ERP) charge intensity calculated electric field strength and receiving peak voltage radiated technique showed in Figure 11. The second technique is to calculate electric field strength as shown in Figures 11 (b). The electric field strength for free space is specified by formula (3):

$$E(dB\mu V/m) = 107 + ERP\ (dBm) - 20Log_{10}\ d\ (m) \qquad (3)$$

somewhere E is intensity of the electric area, ERP is the radiated energy efficient and d is the PD find location.

The average ERP for four changed positions in FSR measurement was $26\ dBm$ and the PD source position was$10\ m$. As a result, when the charge is $5.63\ nC$ which is found from galvanic measurement, the electric field strength is $113\ dB\mu V/m$.

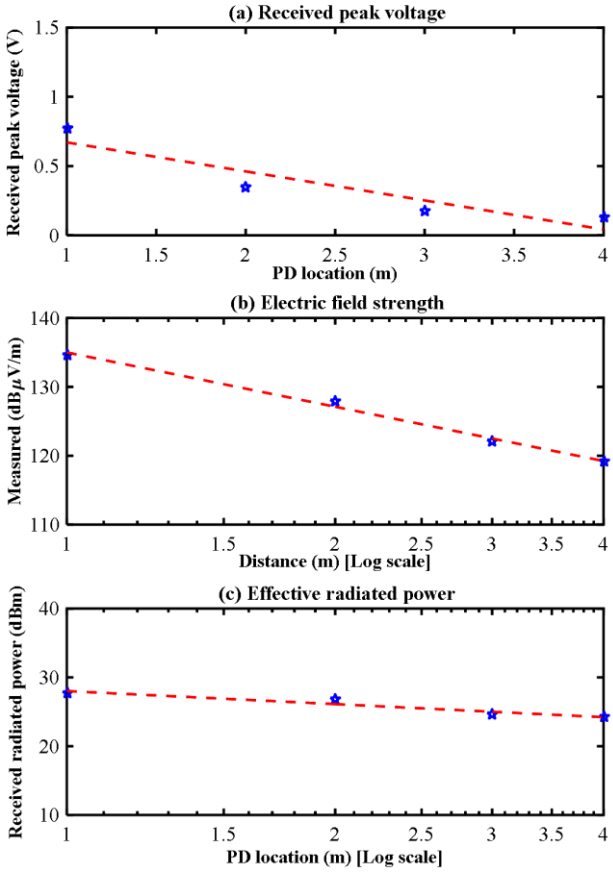

Fig. 11. (a) Received Vp radiated against PD position (b) Electric field strength at various distance. (c) Received radiated power against PD source position.

Table 2 AC HV power source across PD measuring circuit at various distances among PD emulator and antenna.

AC HV source	Galvanic measurement	PD space (m)	Galvanic measurement's mean peak voltage amplitude (V)	Galvanic measurement's mean peak voltage amplitude (dBμV)	(STD) (V)	The integration time of the PD source's first half-cycle (ns)	Charge computed (nC)
15 kV		–	7.19	137.1	1.45	6.4	5.6
	FSR measurement	PD space (m)	FSR measurement's mean maximum voltage magnitude (V)	FSR measurement's mean maximum voltage magnitude (dBμV)	Maximum power of the electric field $dB\mu V/m$	Maximum effective emitted energy dBm	(STD) (V)
		1	0.77	117.7	134.7	27.72	0.306
		2	0.35	110.88	127.9	26.88	0.090
		3	0.179	105.05	122.05	24.55	0.068
		4	0.129	102.2	119.2	24.2	0.035

The floating electrode emulator PD source has been calibrated through injecting pulse of known charge (calibration pulse). The validation waveform simulates a PD occurrence with facts of the case. The charge estimated by averaging a first half of the cycle of the floating electrode emulator PD origins back current (measured charge). For calibration of FSR signals, calculated charge, peak value emitted intensity, and ERP of FSR dimension are checked with place of the emulator PD source. As a result, the charge calculated from the galvanic test looks to be a reasonable estimate to the PD apparent charge.

IV. OUTDOOR FSR TEST AT DIFFERENT DISTANCES

As shown in Table 3 the outdoor test setup results in comparable FSR and therefore the behavior of the peak voltage depending on the PD source location is validated. As seeing in Figure 12, Six places are assigned a unique code dissimilar colure. These shapes demonstration a higher amplitude among the inject charge and the FSR measured peak voltage amplitude signal for each position. In general, it is possible to assert that diverse injected charges and site of a PD emulator source have various qualities in terms of the relationship among the peak voltage of FSR measurement and measured injected charge.

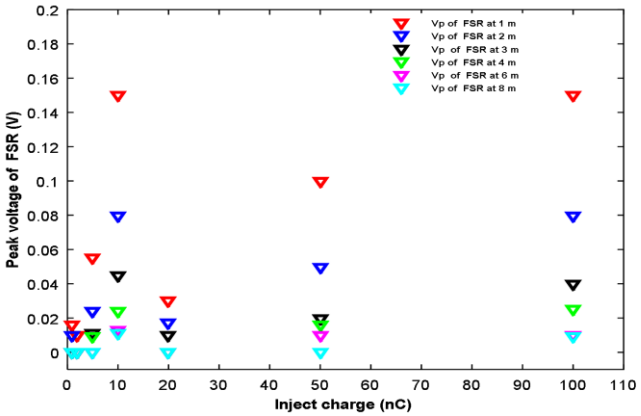

Fig. 12. Correlation between FSR peak amplitude and injected charge at varied PD emulator source places.

V. CONCLUSIONS

Partial discharge signal was captured using galvanic measurement and FSR techniques. The signal was investigated in both the temporal and frequency domains. The results show similarities in time domain signals. The spectrum bands demonstrate that the PD discharge's centre frequency is in the reduced range, in the variety of 50 - 290 MHz. Though, frequency spectra of galvanic and FSR dimensions are not matching with changes in their power distribution. A calibration process was performed. FSR test computed charge, maximum voltage amplitude, and ERP was measured with AC HV power source. The two scenarios of FSR measurement was compared with received Vp radiated and ERP intensity. The ERP radiated intensity of PD FSR measurement pulse will be a known quantity for different distances.

REFERENCES

[1] E. Altshuler and D. Linden, "Design of a wire antenna using a genetic algorithm," Journal of Electronic Defense, vol. 20, pp. 50-52, 1997.

[2] B. Hampton, "UHF diagnostics for gas insulated substations," in High Voltage Engineering. Eleventh International Symposium on (Conf. Publ. No. 467), 1999, pp. 6-16

[3] W. Liming, L. Hong, G. Zhicheng, L. Xidong, and N. Allen, "Sparkover behaviour of air gap with floating electrode combined with impulse and alternating voltages," in Properties and Applications of Dielectric Materials. Proceedings of the 6th International Conference on, 2000, pp. 641-644.

[4] A. Jaber, P. Lazaridis, Y Zhang, D Upton, H Ahmed, U Khan, B Saeed, P Mather, M F Q Vieira, R Atkinson, M Judd, and I A Glover, "Comparison of contact measurement and free-space radiation measurement of partial discharge signals," in Automation and Computing (ICAC), 2015 21st International Conference on 2015,pp. 1-4. IEEE.

[5] J. Guo, E. Shu, and O. Morel, "Partial Discharge calibration using frequency domain measurement in power cables," in Electrical Insulation and Dielectric Phenomena (CEIDP),

[6] 2014 IEEE Conference on, 2014, pp. 200-203.

[7] K.-H. Kim, S.-H. Yi, H.-J. Lee, and D.-S. Kang, "Setup of standard PD calibrator and its uncertainties," Journal of Electrical Engineering & Technology, vol. 6, pp. 677-683, 2011.

[8] A. Cavallini, G. C. Montanari, and M. Tozzi, "PD apparent charge estimation and calibration: A critical review," Dielectrics and Electrical Insulation, IEEE Transactions on, vol. 17, pp. 198-205, 2010.

[9] X.-x. Zhang, J.-z. Tang, J. Tang, Y. Chen, and Y.-b. Xie, "Relationship between UHF PD Detection and Apparent Charge Quantity of Metal Protrusion in Air," Przegląd Elektrotechniczny, vol. 88, pp. 266-270, 2012.

[10] R. Prochazka, K. Draxler, J. Hlavacek, and V. Kvasnicka, "Verification of partial discharge calibrators," in Applied Electronics (AE), 2013 International Conference on, 2013, pp. 1-3.

[11] M. Siegel and S. Tenbohlen, "Comparison between Electrical and UHF PD Measurement concerning Calibration and Sensitivity for Power Transformers," differences, vol. 6, p. 7.

[12] S. Coenen, S. Tenbohlen, S. M. Markalous, and T. Strehl, "Sensitivity of UHF PD measurements in power transformers," Dielectrics and Electrical Insulation, IEEE Transactions on, vol. 15, pp. 1553-1558, 2008.

[13] HVPD. Available: http://www.hvpd.co.uk/ (accessed on November 2015)

[14] E. Lemke, S. Berlijn, E. Gulski, M. Muhr, E. Pultrum, T. Strehl, W. Hauschild, J. Rickmann, G. Rizzi: 'Guide for partial discharge measurements in compliance to IEC 60270', CIGRE Technical Bochure 366, WG D1.33, December 2008

[15] I. E. Commission, High-voltage Test Techniques: Partial Discharge Measurements: International Electrotochnical Commission, 2000.

Table 3 change of peak voltage amplitude of injected charge depending on PD emulator location.

Injected pulse charge across the terminals of PD emulator	Antenna distance from emulator	1 m	2 m	3 m	4 m	6 m	8 m
1 nC	Measured Vp of FSR (V)	0.016	0.010	x	x	x	x
	Vp of FSR pulse ($dB\mu V$)	84	80	x	x	x	x
	Peak electric field strength $dB\mu V/m$	101	97	x	x	x	x
	Peak effective radiated power dBm	-5.9	-4.0	x	x	x	x
2 nC	Measured Vp of FSR (V)	0.010	x	x	x	x	x
	Peak voltage of FSR pulse ($dB\mu V$)	80	x	x	x	x	x
	Peak Electric field strength $dB\mu V/m$	97	x	x	x	x	x
	Peak effective radiated power dBm	-10	x	x	x	x	x
5 nC	Measured Vp of FSR (V)	0.055	0.024	0.01	0.009	x	x
	Peak voltage of FSR pulse ($dB\mu V$)	94.8	87.6	80	79.1	x	x
	Peak Electric field strength $dB\mu V/m$	112	105	97	96.1	x	x
	Peak effective radiated power dBm	4.8	3.6	-0.5	1.08	x	x
10 nC	Measured Vp of FSR (V)	0.15	0.08	0.04	0.024	0.013	0.011
	Vp of FSR pulse ($dB\mu V$)	104	98.1	92.0	87.6	82.3	80.8
	Peak electric field strength $dB\mu V/m$	121	115	109	105	99.3	97.8
	Peak effective radiated power dBm	13.5	14.1	11.5	9.60	7.87	8.82
20 nC	Measured Vp of FSR (V)	0.034	0.017	0.01	x	x	x
	Vp of FSR pulse ($dB\mu V$)	90.6	84.6	80	x	x	x
	Peak electric field strength $dB\mu V/m$	108	102	97	x	x	x
	Peak effective radiated power dBm	0.62	0.61	-0.5	x	x	x
50 nC	Measured Vp of FSR (V)	0.10	0.05	0.02	0.016	0.010	x
	Peak voltage of FSR pulse ($dB\mu V$)	100	93.9	86	84.1	80	x
	Peak electric field strength $dB\mu V/m$	117	111	103	101	97	x
	Peak effective radiated power dBm	10	9.97	5.52	6.08	5.6	x
100 nC	Measured Vp of FSR (V)	0.15	0.08	0.04	0.025	0.010	0.009
	Vp of FSR pulse ($dB\mu V$)	104	98.1	92.0	87.9	80	79.1
	Peak electric field strength $dB\mu V/m$	121	115	109	105	97	96.1
	Peak effective radiated power dBm	13.5	14	11.5	9.95	5.6	7.08